Feasibility study of fissile mass detection in 870 L radioactive waste drums using delayed gamma rays from neutron-induced fission

R. de Stefano, C. Carasco, B. Pérot, E. Simon, T. Nicol, E. Mauerhofer

Feasibility study of fissile mass detection in 870 L radioactive waste drums using delayed gamma rays from neutron-induced fission

R. De Stefano [1], C. Carasco [2], B. Pérot [2], E. Simon [2], T. Nicol [2], E. Mauerhofer [2]

[1] *CEA, DEN, Cadarache, DTN, SMTA, Nuclear Measurement Laboratory, F-13108 Saint-Paul-lez-Durance, France*

[2] *CEA, DEN, Cadarache, DER, SPRC, F-13108 Saint-Paul-lez-Durance, France*

[2] *Forschungszentrum Jülich, Jülich Centre for Neutron Science, D-52425, Jülich, Germany*

Abstract

The measurement of delayed gamma rays following neutron-induced fission is simulated with MCNP 6.1 to investigate the feasibility of fissile material detection in long-lived, medium activity radioactive waste in 870 L. The signal from homogeneously distributed fissile material in the drum is several hundred counts in the main delayed gamma peaks of interest. In a peripheral position or in the drum center, the signal is however too small to allow for a reliable measurement.

Keywords

Delayed gamma, neutron induced fission, long-lived medium activity waste, 870 L radioactive waste drum, MCNP

Introduction

Since the end of the ‘80s, CEA has produced large volume 870 L radioactive waste drums [1] that are stored in Cadarache, France. These legacy drums are filled with wafers corresponding to smaller compacted drums. The fissile mass within the drums needs to be known in order to limit criticality risks during transport, interim storage and in the final repository for which the maximum accepted fissile mass is of the order of 200 g. In practice, only tens of grams of fissile mass are really expected to be present in these drums [2]. The goal of the work presented in this paper is to test the preliminary detectability of some tens of grams of ^{235}U or ^{239}Pu with three different distributions in the 870 L drum by neutron-induced fission delayed gamma rays measurement.

The delayed gamma rays of interest emitted by the fission products of ^{235}U and ^{239}Pu have been identified in previous work mainly presented in [2] and [13]. We select six of these delayed gamma rays for this feasibility study. These delayed gamma rays and their respective fission product and half-life based on LARA nuclear database [3] are reported in Tab. 1. The MCNP 6.1 Activation Control Card (ACT Card) [4] is used to simulate fission delayed gamma rays. As shown in more details in the work presented in [5], the ACT card correctly reproduces the order of magnitude of the experimental net counts obtained by irradiating bare samples (i.e. without waste matrix) of Highly Enriched Uranium (HEU) and Plutonium in REGAIN Prompt Gamma Neutron Activation Analysis (PGNAA) cell of the Nuclear Measurement Laboratory of CEA Cadarache, France. REGAIN was made of graphite walls, a pulsed DT neutron generator and a 33 % HPGe (high purity germanium) detector.

As REGAIN is today dismantled and was only able to accept 120 L waste drums, we decided to perform this feasibility study of fission delayed gamma-ray detectability in 870 L legacy waste drums with the MCNP model of another PGNAA cell called MEDINA (Multi Element Detection based on Instrumental Neutron Activation), located at FZJ in Jülich, Germany. With this MEDINA model, we already studied the detection of neutron-induced fission delayed gamma rays in 225 L waste drums as reported in [6], without the ACT card. In [6], calculation was split in two steps: (1) fission rate followed

by (2) detection of fission delayed gamma rays. In the present study, the ACT card allows simplifying calculation by directly obtaining the fission delayed photon flux at the entrance of the HPGe detector. For the present work, the MCNP model of MEDINA was adapted to accept 870 L drums. The time vs. energy output data from the MCNP calculations (F5:P tally, i.e. photon flux at the detector position) was then processed with MODAR Software (MCNP Output Data Analysis with Root) [7]. This last allows a temporal analysis of gamma rays of interest and the convolution of the photon flux spectra with the response function of a HPGe detector.

γ ray energy	885 keV	1011 keV	1384 keV	1436 keV	1768 keV	2218 keV
Fission fragment	^{104}Tc	^{101}Mo	^{92}Sr	^{138}Cs	^{138}Xe	^{138}Cs
Half-life $T_{1/2}$	18.3 min	14.6 min	2.65 h	33.4 min	14.1 min	33.4 min

Table 1. Main delayed gamma rays emitted by ^{235}U and ^{239}Pu fission fragments for this study.

Validation of the use of MCNP 6.1 Activation Control Card

The study presented in details in [5] consisted in confronting experimental results obtained with REGAIN graphite cell with simulated results. Some of the experiments led during the campaign presented in [6] consisted of interrogating a metallic Highly Enriched Uranium (HEU) or plutonium bare sample of some tens of grams by 14 MeV neutrons emitted by a GENIE 16 neutron generator of 8.10^7 s^{-1} average intensity thermalized in the cell. The HEU and plutonium samples were irradiated for 2 h and were then moved to a low-background spectrometer where the delayed gamma rays were measured with a 25 % relative efficiency HPGe, with sequential spectra acquisitions every 15 min, for a global 24-h measurement time. In the low-background cell, a thin 3 mm lead shield was placed between the fissile materials metallic samples and the HPGe detector in order to limit the signal from the low energy gamma rays of ^{241}Am. The 24-h measurements have been simulated using the models described in [5], taking into account the transfer of the bare samples from REGAIN cell to the low-background cell (1-min transfer). The time chronogram of these experiments is presented in Fig. 1.

All gamma rays from activation of non-nuclear materials in the cell were not calculated by using the option NONFISSION=NONE of ACT Card, thus simulating the low-background cell conditions. The delayed gamma rays calculated with MCNP 6.1 ACT card were studied by analyzing the decay time of non-nuclear activated elements and fission fragments as detailed in [5]. The simulated net counts are calculated for the first 15 min after the end of irradiation by applying the formula in Eq. (1):

$$MCNP_{counts}\,(E) = \int_{t2}^{t3}\left(\int_{E'} F5_{ACT}(E',t) \times RF_{HPGe33\%}(E',E)dE'\right)\,dt.\; T_{irrad}\,.E_n \qquad (1)$$

where t_2 = 1 min is the time transfer from REGAIN to the low-background spectrometer and t_3= 16 min ; $F5_{ACT}$ (E',t) corresponds to the point photon flux obtained at the entrance of the HPGe detector; The response function $RF_{HPGe33\%}$(E',E) corresponds to the probability that a photon with energy E' leads to an energy deposit E in the gamma-ray HPGe detector of 33% relative efficiency; T_{irrad} (s) is the full irradiation time of 2 hours; E_n (n.s^{-1}) is the 8.10^7 n.s^{-1} average neutron emission of the GENIE 16 neutron generator during irradiation. In addition, as MODAR response function corresponds to a 33 % HPGe, we have also calculated the efficiency of the 25 % HPGe used in the low-background spectrometer and we have applied the correction reported in Tab. 2 for each delayed gamma ray. The respective full energy peaks efficiencies are calculated with an isotropic mono-energetic photon point source placed 12.5 cm from both 25 % and 33 % relative efficiency HPGe detectors (like in REGAIN experiment) and a F8:P energy deposition tally in the volume of the respective germanium crystal cells presented in Fig. 2.

In the MCNP net simulated counts in Tab. 3 only statistical uncertainties linked to each computation are reported. Indeed, these numerical simulations have been performed with 5×10^9 source neutrons, which corresponds to a relative statistical uncertainty on each gamma ray present in the F5:P photon flux tally between 1 % and 3 %. However, this figure does not represent the total MCNP calculation uncertainty. Indeed, the uncertainty associated to the fine geometrical description of nuclear material metallic HEU and Pu bare samples in the numerical model might be significant as self-shielding is large in these samples, and extremely geometry-dependent. Calculated self-shielding factors

reported in ref. [6] are 3.8 and 5.7 in the HEU and Pu samples, respectively, but ref. [6] also reports that calculation underestimates the measured fission rates by 55 % and 37 %, respectively. This is probably due to discrepancies between the models and the real geometry of these samples. Indeed, the geometry of the metallic fissile core of these old samples manufactured in the '60s is not known with a good precision and only their outer dimensions (of the zirconium alloy envelope) and masses are well known. In addition, the uncertainties on nuclear data, in particular on fission products yields (leading to delayed gamma ray emissions) are not taken into account. Concerning experimental results reported in Tab. 3, the standard deviation on the net peak area S (number of counts) of a delayed gamma ray is calculated with Eq. 2 (following Poisson law).

$$\sigma = \sqrt{S + 2B} \qquad (2)$$

where B is the Compton continuum background under the peak (number of counts). For the main experimental results σ corresponds to an experimental relative uncertainty of about 10 %, which is much smaller than the uncertainties related to self-shielding which are described above. Calculations and measurements being of the same order of magnitude is however encouraging enough to allow further numerical exploratory investigations using MCNP 6.1 ACT card. Consequently, we will use this delayed gamma-ray calculations method based on MCNP ACT card to study the feasibility of the 870 L drum characterization by the measurement of delayed gamma rays from neutron-induced fission.

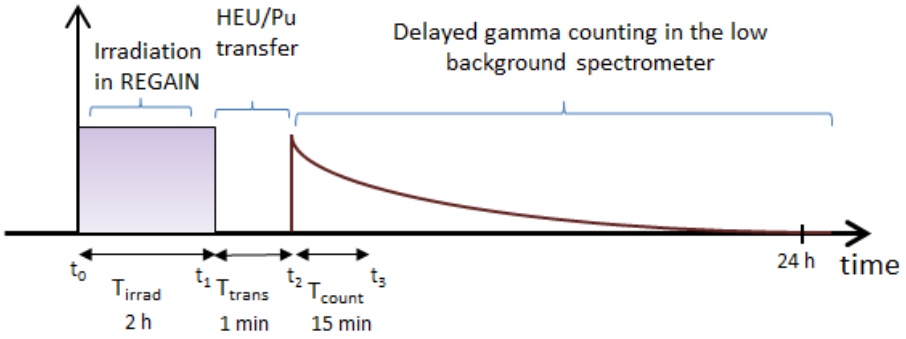

Fig 1: Time chronogram related to the HEU/Pu samples irradiation in REGAIN and delayed gamma measurement in the low-background spectrometer

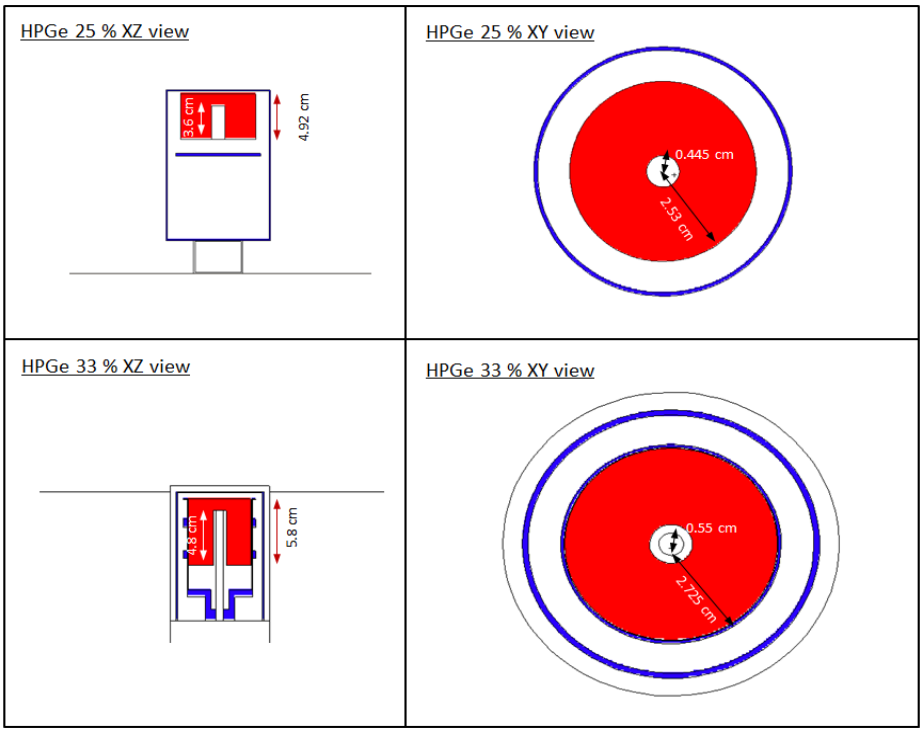

Fig. 2 MCNP models of the 33 % and 25 % relative efficiencies HPGe detectors with their respective germanium crystals (red) and aluminum envelopes (blue). Note that the XZ and XY views are not at the same scale.

γ ray energy	885 keV	1011 keV	1384 keV	1436 keV	1768 keV	2218 keV
Efficiency for a HPGe 25%	1.471×10^{-3}	1.334×10^{-3}	1.014×10^{-3}	0.982×10^{-3}	0.820×10^{-3}	6.582×10^{-4}
Efficiency for a HPGe 33%	1.875×10^{-3}	1.686×10^{-3}	1.317×10^{-3}	1.277×10^{-3}	1.054×10^{-3}	0.880×10^{-3}
Correction factor	**0.784**	**0.791**	**0.770**	**0.769**	**0.778**	**0.748**

Table 2. Detection efficiencies of the 33 % and 25 % HPGe detectors calculated with MCNP (see models in Fig. 2) for a gamma point source located at 12.5 cm from the detector entrance surfaces as in the experiment.

γ ray energy	885 keV	1011 keV	1384 keV	1436 keV	1768 keV	2218 keV
Experimental net counts with U	790 ± 67	918 ± 98	612 ± 40	1211 ± 54	172 ± 25	102 ± 24
MCNP 6.1 net counts with U	648 ± 8	744 ± 23	597 ± 10	877 ± 12	183 ± 4	130 ± 3
Experimental net counts with Pu	1464 ± 106	760 ± 66	347 ± 36	1057 ± 48	102 ± 29	198 ± 37
MCNP 6.1 net counts with Pu	873 ± 6	552 ± 14	238 ± 3	567 ± 4	118 ± 2	85 ± 1

Table 3 Simulated net counts **vs**. experimental net counts of the main delayed gamma rays of interest from HEU and plutonium samples after a 15-min measurement following a 2-h irradiation in the REGAIN neutron interrogation cell.

MCNP model of the measurement cell for the 870 L drums

The graphite cell used for this study is based on an existing MCNP model of the MEDINA facility of the Forschungszentrum Jülich (FZJ) described in [6] [8] [9]. As MEDINA was built with the aim of detecting toxic chemicals in up to 225 L drums the model of this MEDINA cell has been slightly modified by enlarging the interrogation cavity to accept the 870 L waste drum. A graphite block has also been added in the bottom of the cell to limit neutron leakages to the ground. In the same way, the graphite roof of the cell has been enlarged to limit neutron leakage in the top corners of the cell and thus improve the thermal neutron flux and hence fissile mass interrogation. The new model of the cell named MEDINA 2 is presented in Fig. 3.

As MEDINA cell, MEDINA 2 is modelled with high purity graphite blocks allowing the 14 MeV fast neutron thermalisation. The composition of this graphite blocks used for this model is reported in Tab. 4. An isotropic 14 MeV neutron point source is simulated with a 10^{10} s^{-1} intensity (corresponding to a GENIE 35 neutron generator of SODERN). Note that the original 104 % relative efficiency HPGe of MEDINA is replaced by a 33 % HPGe, the response function of this detector being available in MODAR for time-energy investigations. For the first study, 10 g of ^{235}U or ^{239}Pu were simulated with a

homogenous distribution in the five compacted drums filling the 870 L drum, meaning 2 g per wafer. The detailed description of the 870 L drum geometry and materials is given in [2]. For the second and third case studies corresponding to heterogeneous fissile materials, two metallic 10 g ^{235}U and ^{239}Pu spheres (radius ≈ 0.5 cm) were simulated at the edge and in the center of the third wafer. Spheric shapes are chosen as simplification, in order to avoid anistropic self-attenuation effects within the sample.

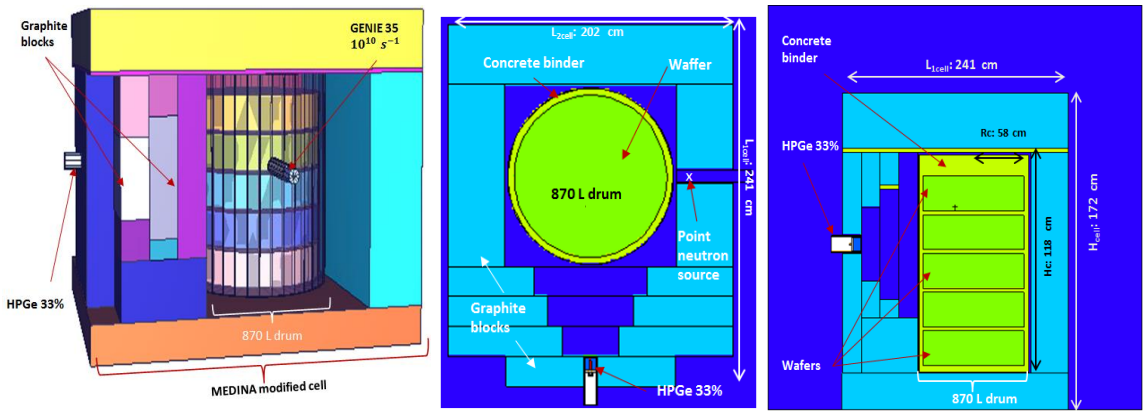

Fig. 3. 3D view (left), horizontal cross section (middle) and vertical cross section (right) of the MEDINA 2 graphite cell with a 870 L drum.

Element	% Weight	Element	% Weight	Element	% Weight
^{12}C	99.913	^{1}H	4.05×10^{-3}	^{46}Ti	3.28×10^{-4}
^{40}Ca	1.09×10^{-2}	^{54}Fe	2.93×10^{-4}	^{47}Ti	2.99×10^{-4}
^{42}Ca	1.27×10^{-4}	^{56}Fe	4.59×10^{-3}	^{48}Ti	3.03×10^{-4}
^{43}Ca	2.73×10^{-5}	^{57}Fe	1.10×10^{-4}	^{49}Ti	2.26×10^{-4}
^{44}Ca	5.58×10^{-4}	^{58}Fe	1.40×10^{-5}	^{50}Ti	2.21×10^{-4}
^{48}Ca	3.71×10^{-4}	^{35}Cl	1.52×10^{-4}	^{10}B	3.70×10^{-5}
^{32}P	1.09×10^{-2}	^{37}Cl	4.87×10^{-5}	^{11}B	1.49×10^{-4}
^{33}P	8.63×10^{-5}	^{51}V	3.50×10^{-4}		
^{34}P	4.84×10^{-4}	^{27}Al	4.05×10^{-2}		

Table 4: Graphite blocks composition for the model of the MEDINA2 measurement cell for the 870 L drums

MCNP calculations for a homogeneous distribution of fissile materials

The delayed gamma ray spectra emitted by 10 g of fissile masses homogenously distributed in the five compacted drums are shown in Fig. 4 for both ^{235}U and ^{239}Pu. The main high energy delayed gamma rays of interest from uranium and plutonium (reported in Tab. 1) are present in both spectra. With the aim of being closer to realistic practical measurement of these drums, the net number of counts in these peaks has been simulated for a 3-h acquisition time following the end of the 2-h irradiation, see Tab. 5. The MCNP net number of counts for this study are calculated following Eq. (1) with t_2 = 1 min and t_3 = 3 hours.

Tab. 5 reports statistical uncertainties on the net peak area (number of counts S after subtraction of the Compton continuum background B in the HPGe gamma spectrum

simulated with MCNP) of the delayed gamma rays of interest, calculated following Eq. (2).

In addition, in order to calculate detection limits, the active background spectrum corresponding to the activation of the 870 L waste package materials with the NONFISSION = P option of the ACT card has been calculated. The same conditions as for the fission delayed gamma ray useful signal have been used (neutron generator emission, irradiation and counting time). The calculated activation background spectrum reported in Fig. 5 shows no interference between delayed gamma rays of interest for this study and activation gamma rays from the 870 L waste drum. However, the useful signal spectrum of fission delayed gamma rays is 1 to 2 orders of magnitude smaller than the active background spectrum (see Fig. 4 vs. Fig. 5, respectively). Detection Limits (DL in counts) are calculated following Eq. (3), which corresponds to a non-detection risk and a false-alarm risk α=2.5 % and β=2.5 %, respectively [10]:

$$DL\,(E) \approx 3{,}92.\sqrt{2.B_{active\ background}(E)} \qquad (3)$$

where $B_{active\ background}\ (E)$ corresponds to Compton continuum (counts) of the active background spectrum evaluated in the region of interest of each fission delayed gamma ray (energy E), the width of which is between 7 and 8 keV depending on the peak. DL is then divided by the useful signal sensitivity, noted $S_{U/Pu}$ (in g^{-1}), which corresponds to the net counts reported in Tab. 5 per fissile mass unit (U or Pu). The number of counts for the 870 L drum active background continuum and the detection limits in grams for a fissile mass homogeneous distribution in the 5 wafers of the 870 L drum are reported in Tab. 6.

For this 2-h irradiation and 3-h measurement, depending on the delayed gamma ray of interest, detection limits vary between 31.6 g and 123.4 g of ^{235}U, or between 24.1 g and 109.7 g of ^{239}Pu homogeneously distributed in the drum.

γ ray energy	885 keV	1011 keV	1384 keV	1436 keV	1768 keV	2218 keV
Net area for ^{235}U (counts)	397 ± 24	265 ± 19	308 ± 22	395 ± 23	83 ± 11	90 ± 12
Net area for ^{239}Pu (counts)	656 ± 39	412 ± 33	280 ± 23	524 ± 26	90 ± 11	102 ± 11

Table 5 Net counts in the main fission delayed gamma rays calculated with MCNP for a 3-h measurement after the end of the 2-h neutron irradiation, for 10 g of ^{235}U and ^{239}Pu homogeneously distributed in the 870 L drum.

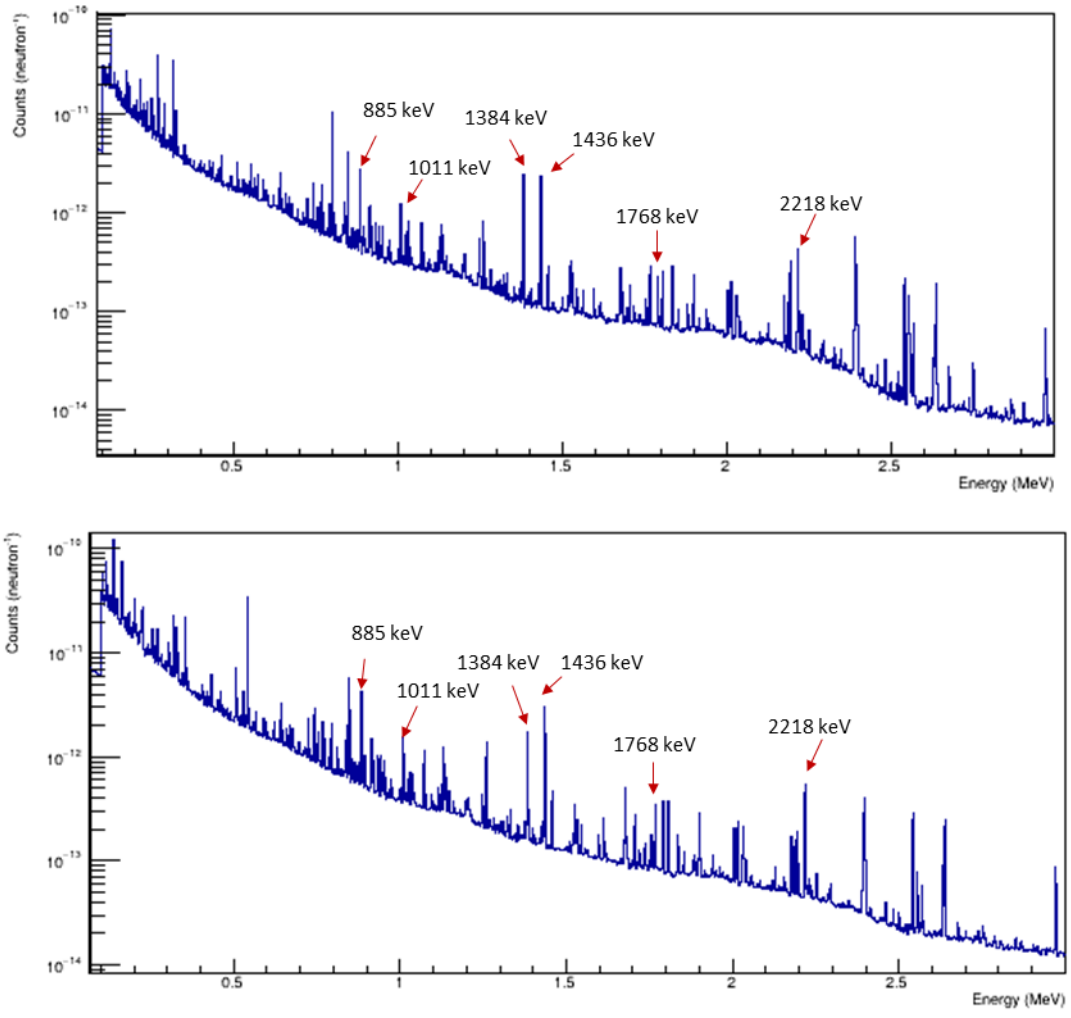

Fig. 4 MCNP simulated spectra obtained for a 3-h measurement after a 2-h irradiation of a 870 L drum containing 10 g of homogenously distributed ^{235}U (above) and ^{239}Pu (below).

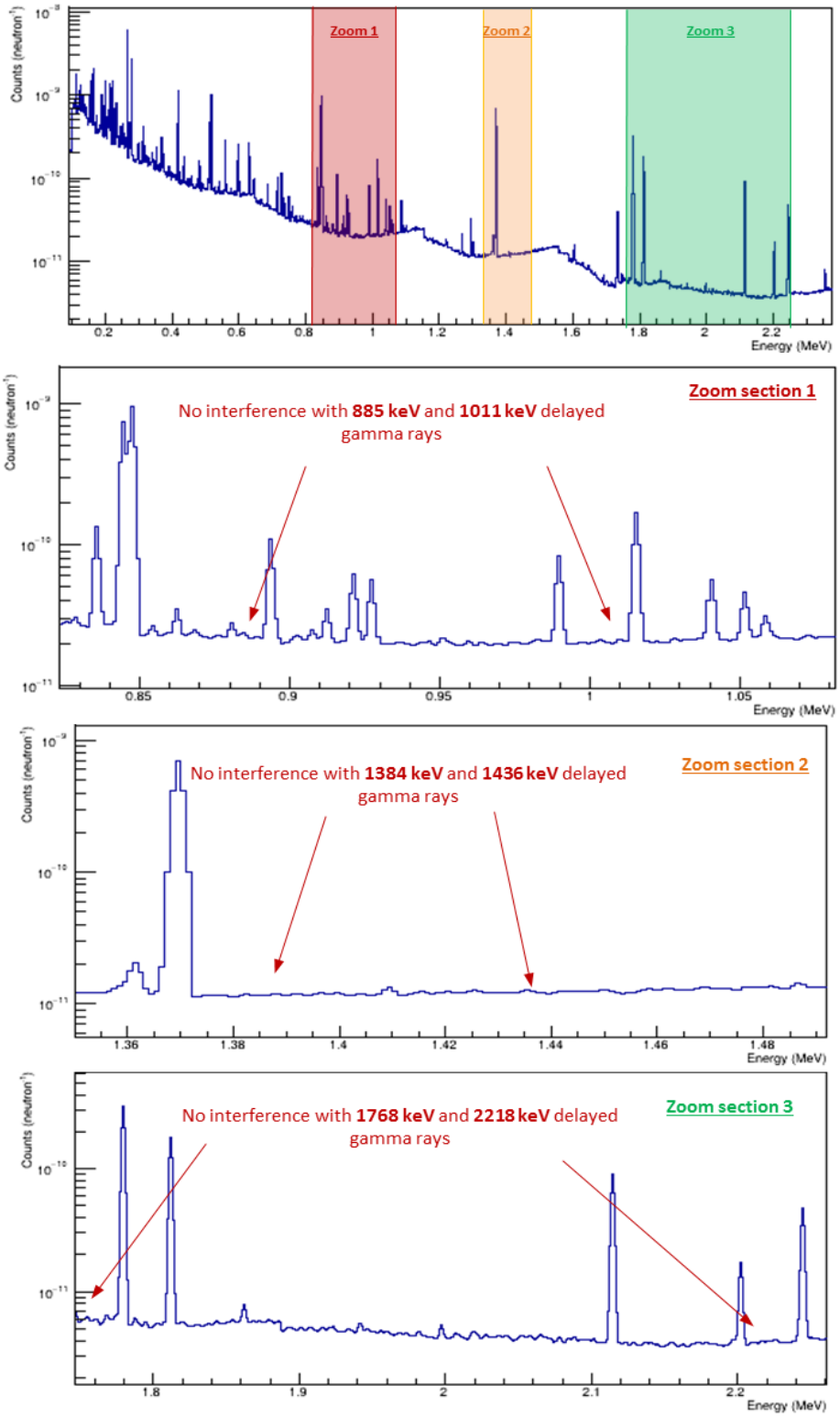

Fig. 5 Simulated active background spectra for a 3-h measurement with a HPGe of 33 % relative efficiency detector after a 2-h irradiation of a 870 L drum, and corresponding zoom sections

γ ray energy	885 keV	1011 keV	1384 keV	1436 keV	1768 keV	2218 keV
DL (in counts)	1928	1882	1457	1262	987	729
DL in ^{235}U mass (g)	48.2	69.7	47.0	31.6	123.4	81.0
DL in ^{239}Pu mass (g)	29.4	45.7	52.0	24.1	109.7	71.5

Table 6 Detection limits of ^{235}U and ^{239}Pu homogeneously distributed in the 870 L drum for each delayed gamma ray of interest.

MCNP calculations for a peripheral distribution of fissile materials

The second study corresponds to a 10 g sphere of ^{235}U or ^{239}Pu located in a peripheral position, i.e. 1 cm from the edge of the third middle wafer. Four positions with respect to neutron generator and detector have been studied: 0°, 90°, 180° and 270° as shown in Fig. 6. The results obtained for 10 g of ^{235}U or ^{239}Pu placed at the edge of the drum are reported in Tab. 7 and Tab. 8, respectively. For each angle, irradiation time is 2 h. The net counts obtained for both uranium and plutonium in 0° and 270° positions are much smaller than with a homogenous distribution, and the signal is not detectable in the 90° and 180° positions. This is mainly due to neutron self-shielding and gamma self-absorption inside the thick nuclear material spheres (1 cm in diameter), and to combined matrix-position effects leading also to large neutron and gamma attenuation in the 870 L waste materials. Detection limits have also been estimated following Eq. (3) for a peripheral distribution at 0° and 270° with respect to the neutron generator, and are reported in Tab. 9. Detection limits are too high (dozens or hundreds of grams) to envisage a practical application of the method for these drums.

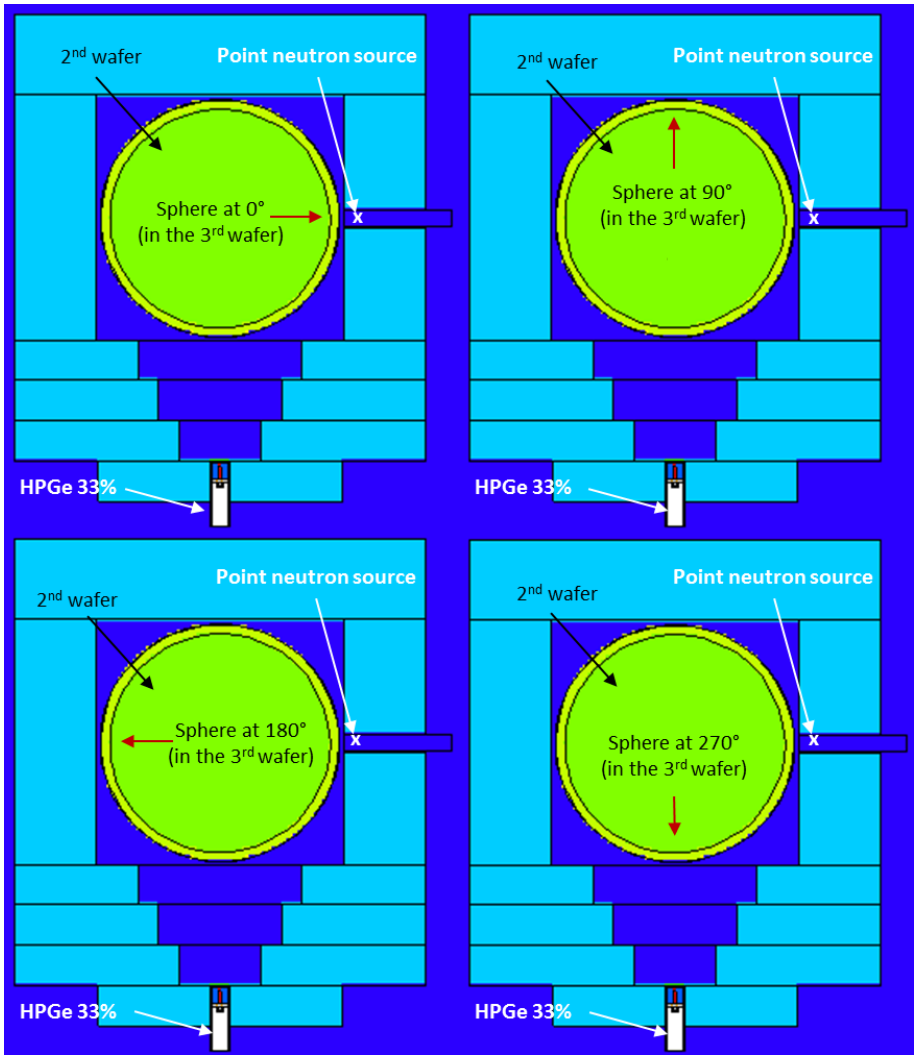

Fig. 6 XY view of MEDINA 2 cell and the 870 L drum with a 10 g fissile material sphere placed at the following irradiation angles with respect to neutron generator: 0°, 90°, 180° and 270°.

γ ray energy	885 keV	1011 keV	1384 keV	1436 keV	1768 keV	2218 keV
Net area at 0° (counts)	39 ± 11	60 ± 9	74 ± 11	64 ± 10	13 ± 5	14 ± 5
Net area at 90° (counts)	< 1	< 1	< 1	< 1	< 1	< 1
Net area at 180° (counts)	< 1	< 1	< 1	< 1	< 1	< 1
Net area at 270° (counts)	145 ± 16	115 ± 12	126 ± 14	167 ± 18	30 ± 7	31 ± 7

Table 7 Net counts for a 3-h measurement after the end of the 2-h neutron irradiation for the main delayed gamma rays of 10 g of ^{235}U placed at the edge of the 870 L drum.

γ ray energy	885 keV	1011 keV	1384 keV	1436 keV	1768 keV	2218 keV
Net area at 0° (counts)	188 ± 33	77 ± 20	72 ± 11	90 ± 12	20 ± 5	22 ± 5
Net area at 90° (counts)	< 1	< 1	< 1	< 1	< 1	< 1
Net area at 180° (counts)	< 1	< 1	< 1	< 1	< 1	< 1
Net area at 270° (counts)	233 ± 25	128 ± 17	122 ± 13	161 ±14	25 ± 6	30 ± 6

Table 8 Net counts for a 3-h measurement after the end of the 2-h neutron irradiation for the main delayed gamma rays of 10 g of ^{239}Pu placed at the edge of the 870 L drum.

γ ray energy	885 keV	1011 keV	1384 keV	1436 keV	1768 keV	2218 keV
DL in ^{235}U mass (g) at 0°	494	313	197	197	760	520
DL in ^{239}Pu mass (g) at 0°	102	250	202	140	494	331
DL in ^{235}U mass (g) at 270°	133	164	115	76	329	235
DL in ^{239}Pu mass (g) at 270°	83	147	119	78	394	243

Table 9 Detection limits (grams) of ^{235}U and ^{239}Pu located in the 870 L drum at 0° and 270° with respect to the neutron generator, for each delayed gamma ray of interest.

MCNP calculations with fissile materials in the drum center

The third case study consists of fissile material placed in the drum center, in the middle of the third wafer as shown in Fig. 7. The results obtained for a 2 h drum irradiation followed by a 3 h counting measurement for the ^{235}U and ^{239}Pu spheres are reported in Tab. 10. In this configuration, for each high energy delayed gamma ray of interest from uranium and plutonium, the net number of counts is lower than 10 and it is clear that detecting 10 g of fissile masses in the center of a 870 L drum is not possible. Note that detection limits have not been calculated for this section as the net counts signal from delayed gamma rays of interest is hardly detectable. Indeed, the performances of the method are intrinsically very poor due to the attenuation of the interrogating neutron flux

in the concrete envelope of the 870 L drum. Therefore, another method based on delayed gamma rays induced by photo-fission with high energy X-rays (produced by a 15 MeV electron LINAC) is also currently under study at CEA, which shows more encouraging results for nuclear materials detection in 870 L waste drums [2] [11] [12].

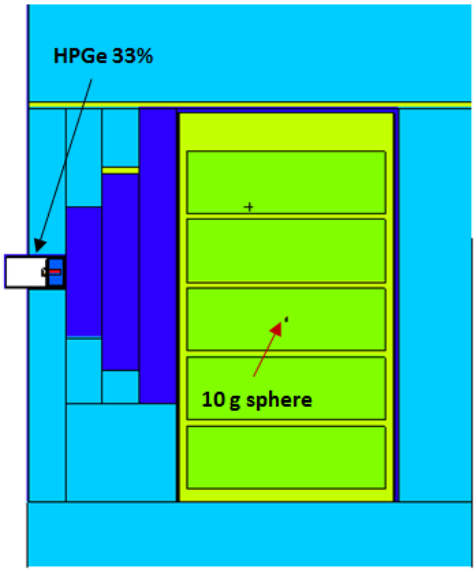

Fig. 7 Vertical cross section of MEDINA 2 cell showing the 870 L drum with a 10 g fissile material sphere placed in the center.

γ ray energy	885 keV	1011 keV	1384 keV	1436 keV	1768 keV	2218 keV
Net area for ^{235}U (counts)	3 ± 2	2 ± 1	7 ± 4	2 ± 1	2 ± 1	2 ± 1
Net area for ^{239}Pu (counts)	7 ± 4	5 ± 3	5 ± 3	7 ± 3	1 ± 1	2 ± 1

Table 10 Net counts in the main fission delayed gamma rays, for a 3-h measurement after the end of the 2-h neutron irradiation, for 10 g of ^{235}U and ^{239}Pu placed at the 870 L drum center.

Conclusion and prospects

This feasibility study explored the detectability of ^{235}U or ^{239}Pu in 870 L legacy CEA drums by means of neutron activation analysis and neutron-induced fission delayed gamma measurements. For this purpose, a graphite cell has been modeled with MCNP 6.1 and the net counts in the main delayed gamma rays of interest have been calculated

for different fissile masses distributions, for a 3-h measurement with an HPGe detector of 33 % relative efficiency following a 2-h irradiation with a neutron source of 10^{10} s^{-1}. Results are encouraging for fissile materials homogeneously distributed in the waste, with detection limits between 31.6 and 123.4 grams of ^{235}U, or between 24.1 and 109.7 grams of ^{239}Pu for the main high energy delayed gamma rays of interest. However, in case of small samples of fissile materials located in periphery of the drum, the net counts are much smaller due to both self-shielding and combined matrix-position effects and detection limits are too high for a practical application to 870 L drums. Finally, if the samples are located in the center of the drum, it is effectively impossible to detect any delayed gamma ray of interest.

The signal could be increased by using a detector with higher efficiency, such as the 104 % HPGe detector used in MEDINA cell [6], and by implementing several HPGe detectors around the 870 L drum. The acquisition could also be performed between the pulses of the neutron generator (instead of after irradiation only) to increase the delayed gamma counting time.

References

1. Inventaire national des matières et déchets radioactifs – Catalogue descriptif des familles Andra (2015).https://www.andra.fr/download/site-principal/document/editions/559.pdf. Accessed 09 Apr. 2019

2. E. Simon et. al. (2016) Feasibility study of fissile mass quantification by photofission delayed gamma rays in radioactive waste packages using MCNPX, Nucl. Instr. Meth. A, 840:28‑35, déc. 2016.

3. "NUCLEIDE-LARA on the web (2018)" [online] available on: http://www.nucleide.org/Laraweb/index.php

4. J. W. Durkee (2012) MCNP6 Delayed-Particle Verification And Validation Rev 5, LA-UR-12-00676

5. R. De Stefano et. al. (2019), Simulation of U/Pu induced fission delayed gamma rays with MCNP 6, To be published in Nuclear instrumentation and measurement methods in nuclear environments conference records (ANIMMA), June 2019.

6. T. Nicol et al. (2016), Feasibility study of 235U and 239Pu characterization in radioactive waste drums using neutron-induced fission delayed gamma rays », Nucl. Instr.. Meth. Phys. A, 832:85‑94.

7. C. Carasco (2010) MCNP output data analysis with ROOT (MODAR) », Comp. Phys. Com., v181:2210‑2211.

8. T. Nicol, et. al. (2016) HPGe-detector shielding optimization with MCNP for the MEDINA neutron activation cell, J Radioannal Nucl Chem 310:865‑874.

9. T. Nicol et al. (2016), Quantitative comparison between PGNAA measurements and MCNPX simulations », J Radioannal Nucl Chem. 308:671‑677.

10. G. Gilmore, Practical Gamma-ray Spectroscopy, second edition, Wiley, 2008.

11. F. Carrel et al. (2010), Identification and Differentiation of Actinides Inside Nuclear Waste Packages by Measurement of Delayed Gammas, IEEE Trans. Nucl. Sci., 57:2862‑2871.

12. E. Simon et. al. (2016) Fissile mass quantification in radioactive waste packages using photofission delayed gamma rays, IEEE Nucl. Sci. Symp., Med. Imag. Conf. and Room-Temp. Semicond. Det. Workshop (NSS/MIC/RTSD), 1‑4

13. F. Carrel et al. (2011) New Experimental Results on the Cumulative Yields From Thermal Fission of ^{235}U and ^{239}Pu and From Photofission of ^{235}U and ^{238}U Induced by Bremsstrahlung, IEEE Trans. Nucl. Sci., 58:2064‑2072.